Microstructure of Ionomers: Interpretation of Small-Angle X-ray Scattering Data

David J. Yarusso and Stuart L. Cooper*

Department of Chemical Engineering, University of Wisconsin, Madison, Wisconsin 53706.
Received October 27, 1982

ABSTRACT: The interpretation of the small-angle X-ray scattering (SAXS) data for ionomers has been the subject of considerable controversy in recent years. In this work, SAXS absolute scattered intensity data without slit-smearing effects have been obtained on a series of sulfonated polystyrene ionomers. The various microstructure models that have been proposed are evaluated by fitting calculated SAXS curves for each of the models to these data. It is shown that none of the existing models is entirely satisfactory. A new model is proposed that attributes the scattering peak to interference between small ionic aggregates arranged with a liquid-like degree of order in the material. The model is a variation on the model of a system of hard spheres in which the closest approach radius is larger than the scattering particle radius. The model provides an excellent fit to the data and is consistent with the sample compositions. The interpretation of other data regarding the dependence of the SAXS curve on swelling and stretching of the sample and the existence of two different ion environments is discussed.

I. Introduction

The term "ionomer" has been applied to copolymers consisting primarily of hydrophobic repeat units with a small fraction of the monomer units containing ionic functionality either on pendant groups or in the main chain. This is most often a salt of a carboxylic or sulfonic acid group. Research on the microstructure of ionomers has been extensive over the past few years because of the unique physical properties that these materials possess. Some examples of ionomers that have found commercial application are Surlyn and Nafion, both manufactured by E. I. du Pont de Nemours. Surlyn is a copolymer of ethylene and methacrylic acid containing less than 10 mol % methacrylic acid and neutralized with Zn^{2+} or Na^{+}. This material has a high melt strength and excellent toughness and is optically clear, making it ideal for certain packaging applications.[1] Nafion, on the other hand, is important because of its transport properties. This ionomer consists of a poly(tetrafluoroethylene) backbone with occasional perfluoro ether side chains terminated by sulfonic acid groups. Because of its hydrophilicity, selective permeability to cations, low resistance to current flow, and excellent chemical stability, Nafion has been used as a separation membrane material in chlor-alkali electrochemical cells.[2]

Although very different, the unique properties of both Surlyn and Nafion appear to be due in some way to aggregation of the ionic species in these systems. Much research has been directed toward more fully understanding the microstructure of ionomers in order to rationalize their physical properties. Although the existence of ion aggregates is generally recognized, the basic questions of their size, internal structure, and distribution in the material are still matters of considerable uncertainty. A detailed discussion of these issues and a review of the work in this area is given in a paper by MacKnight and Earnest[3] and in two recent books.[4,5]

Several models of the microstructure of ionomers have been proposed, some based primarily on the interpretation of mechanical and spectroscopic data and some based on the analysis of small-angle X-ray scattering (SAXS) data. Eisenberg postulated the existence of two types of ion aggregation, which were termed multiplets and clusters.[4,6,7] These designations were based on certain apparent transitions in the behavior of ionomers as the ion content is increased. A multiplet is a group of a few ion pairs (no more than about eight) tightly aggregated and excluding all hydrocarbon material. If the multiplets are assumed to be spherical, geometric constraints limit their size to about 0.6 nm in diameter.[7] At higher ion contents, Eisenberg suggests the formation of clusters. Clusters are defined as groups of several multiplets that form a domain in the material which is locally rich in ionic material but contains a significant amount of hydrocarbon as well. The size of these entities is presumed to be on the order of 5–10 nm in diameter. Several spectroscopic experiments, including dielectric, infrared, and Raman measurements, have indicated that there are two different ion environments, and these have usually been interpreted as corresponding to multiplets and clusters.[8–11]

The earliest and most direct evidence for the existence of ion aggregation in ionomers was the appearance of a peak in the SAXS pattern of an ethylene/methacrylic acid copolymer upon neutralization with Na^{+}.[12] This characteristic peak has since been observed in many ionomer systems. In ionomers based on carboxylic acid, the peak appears only in the neutralized form of the polymer but not in the acid form.[13–17] In sulfonic acid based ionomers, however, the peak may be observed in the acid form as well.[18–21,49] Figure 1 shows data obtained by the authors for 6.9% sulfonated polystyrene neutralized 85% with Zn^{2+}. The curve is typical of ionomer SAXS data. The characteristic ionomer SAXS peak is broad and centered at q values ranging from 1.5 to 2.5 nm^{-1} for different ionomers. ($q = 4\pi/\lambda$) sin θ, where 2θ is the scattering angle and λ is the X-ray wavelength.) If Bragg's law is applied to the peak positions, the corresponding spacings are 2.5–4.0 nm. If the measurements are made at low enough angles, one usually observes an upturn in intensity like that seen in Figure 1. In ionomers with crystallizable backbones, one may also observe another peak at a lower q value than the characteristic ionomer peak that arises from scattering from crystalline lamellae. Roche et al.[22] studied the deformation dependence of the apparent Bragg spacing (d_B) in the directions parallel and perpendicular to elongation in ethylene/methacrylic acid ionomers. They found that the d_B values changed much less than the macroscopic sample dimensions. Several studies[14,20,23] have shown that upon swelling of the ionic domains with polar solvents, d_B increases, but much more than the macroscopic linear dimensions.

Various microstructural models have been proposed to explain these SAXS observations. They differ primarily in whether they attribute the peak to interference between different ionic aggregates or to an internal structure of the aggregate. Very few attempts have been made to check

0024-9297/83/2216-1871$01.50/0

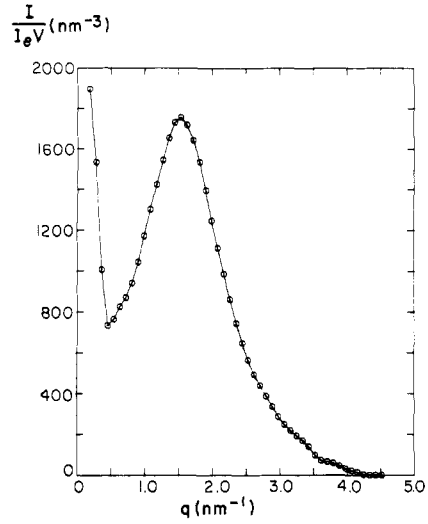

Figure 1. SAXS data for zinc-neutralized sulfonated polystyrene ionomer (sample 4D).

the quantitative agreement of these models with experimental data. Most of the arguments for or against different models have been made on the basis of certain qualitative characteristics of the model and the data so that the question is still far from resolved. In addition, the correlation between the various SAXS models and the multiplet–cluster concept has not been clear.

In order to better evaluate the various models, we considered it necessary to obtain absolute intensity SAXS data on a simple, well-characterized ionomer system. Sulfonated polystyrene was chosen because there is no possibility of backbone crystallinity and because the post-polymerization sulfonation procedure is likely to produce a nearly random placement of sulfonate groups. Using such data, we will show in this work that none of the existing models is entirely consistent with the data. A new model is proposed that can very accurately model the SAXS curve with the exception of the upturn in intensity near zero angle. The model parameters are consistent with the sample compositions. In addition, the existence of two ion environments can be interpreted in terms of the proposed model.

II. Experimental Section

Four samples of partially sulfonated polystyrene prepared according to the procedure described elsewhere[24,25] were obtained from Dr. Robert Lundberg and the late Dr. Henry Makowski of Exxon Research and Engineering Co. The chemical structure of these materials is

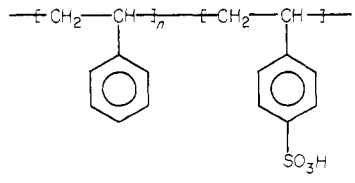

Atomic absorption analysis was used to determine the degrees of sulfonation of the four different samples. The polymers were dissolved in a 60/40 mixture by volume of toluene and dimethyl sulfoxide (Me_2SO) at a concentration of 100 g/L. The solutions were filtered through no. 1 filter paper using nitrogen pressure.

The filtered solutions were then neutralized to three different levels by dissolving the desired amount of zinc acetate dihydrate in a minimum amount of water and adding that solution to the polymer solution and stirring for approximately 30 min. The mixture was optically transparent and slightly yellow as was the acid solution. Thus, with this solvent and salt system, a one-phase neutralization is possible. Since only a stoichiometric amount of salt (or less) is used and since the sulfonic acid group is a considerably stronger acid than acetic acid, there is little chance that any Zn^{2+} will be trapped in the polymer in the acetate form.

Table I

sample	mole fraction of sulfonated repeat units	fraction of sulfonate groups neutralized by Zn^{2+}	density, g/cm³
1A	0.0168	0	1.048
1B	0.0337	0	1.045
1C	0.0555	0	1.075
1D	0.0691	0	1.080
2A	0.0168	0.28	1.063
2B	0.0337	0.25	1.077
2C	0.0555	0.24	1.095
2D	0.0691	0.23	1.100
3A	0.0168	0.45	1.066
3B	0.0337	0.46	1.080
3C	0.0555	0.50	1.095
3D	0.0691	0.55	1.102
4A	0.0168	0.86	1.067
4B	0.0337	0.84	1.082
4C	0.0555	0.88	1.102
4D	0.0691	0.85	1.113

After neutralization, the polymer was recovered by pouring the solution into boiling water purged with steam. The steam strips away the toluene, and the Me_2SO dissolves in the water, leaving the polymer as a porous cake on the surface. The polymer cakes were then pulverized in a blender containing a 50/50 mixture of water and methanol to extract residual solvent. The granules were separated from the liquid by filtration and dried in air at 50 °C for 24 h and then under vacuum at 65 °C for 24 h.

The dried granules were then compression molded into disks at 200 and 150 °C for the salt and acid forms, respectively, with an applied pressure of 17 MPa for 10 min. The disks were then annealed and dried under vacuum at 120 °C for 24 h and slowly cooled under vacuum over a period of about 4 h to room temperature. The effect of annealing at higher temperatures was not investigated.

X-ray absorption spectra were obtained in the vicinity of the zinc K edge, and the change in absorption coefficient at the edge relative to the background was used to determine the mass fraction of zinc in the materials and thus the degree of neutralization.[26] The sample densities were measured by buoyancy in Dow Corning Silicone 200 fluid. Table I summarizes the sample designations and chemical characterization data.

SAXS data were obtained with the pinhole collimation camera and two-dimensional position-sensitive detector at Oak Ridge National Laboratory. A sample-to-detector distance of 1.12 m and a pinhole diameter of 1 mm were used. The measurements were performed with Cu Kα radiation from a rotating-anode source operating at 42 kV and 50 mA. Monochromatization was achieved by Bragg diffraction from a graphite crystal. Data were obtained over a q range from 0.1 to 4.5 nm^{-1} with a resolution of about 0.1 nm^{-1}. The data were corrected for detector sensitivity, dark current, parasitic scattering by the camera, and absorption of the beam by the sample. The resulting curves were converted to absolute scattering power by comparison to the scattering from a calibrated Lupolen standard.[27] The data are presented as I/I_eV, where I is the scattered intensity, I_e is the intensity scattered by a single electron under identical conditions, and V is the irradiated sample volume.

Short-range electron density fluctuations and thermal density fluctuations give rise to a broad amorphous halo centered in the wide-angle region which extends into the small-angle region. In order to subtract out this contribution, data were obtained on a Picker wide-angle diffractometer. The curves were normalized to match the SAXS curves in the region of q overlap. The wide-angle data in the q region from 3.9 to 6.7 nm^{-1} were fit by using the exponential form suggested by Rathje and Ruland,[28] and the extrapolated curve was subtracted from the SAXS data.

III. SAXS Background

Small-angle X-ray scattering measurements are used to study heterogeneities in matter having a length scale on

the order of 1–100 nm. If a monochromatic beam of X-rays illuminates a sample and the scattered intensity is measured as a function of scattering angle, it is well-known[29] that the intensity distribution is given by

$$I(\mathbf{q}) = I_e(\mathbf{q})\left[\int_V \rho(\mathbf{r}) e^{-i\mathbf{q}\cdot\mathbf{r}}\, d\mathbf{r}\right]^2 \quad (1)$$

where $\mathbf{q}$ is the scattering wavevector whose magnitude is given by

$$q = (4\pi/\lambda)\sin\theta \quad (2)$$

in which 2θ is the angle between the incident and scattered beams and λ is the radiation wavelength. The direction of $\mathbf{q}$ is the same as that of the vector which is the difference between a unit vector in the scattered direction and one in the incident direction. The vector $\mathbf{r}$ is a position vector and $\rho(\mathbf{r})$ is the electron density distribution in the sample. I_e is the intensity scattered by a single electron under the experimental conditions and I is the observed intensity. The three-dimensional Fourier transform integral is taken over the volume of the sample illuminated by the X-ray beam, V. The Fourier transform is a complex quantity and its square is defined as the result of multiplication by its complex conjugate. Although the Fourier transform is a completely invertible procedure, the squaring causes certain information about the electron density distribution to be lost. Thus, while the intensity profile can, in principle, always be calculated for any microstructure, the reverse procedure is not possible.

Since the small-angle region of the scattering pattern contains the low-frequency components of the fluctuations of $\rho(\mathbf{r})$, it is primarily composed of contributions from the larger scale microphase morphology. The wide-angle region contains primarily contributions from fluctuations in density from atom to atom. Thermal density fluctuations have a variety of wavelengths and contribute to the entire scattering curve. As a consequence, to extract only the information about the phase morphology, one must attempt to subtract the contributions from short-wavelength intraphase fluctuations and thermal density fluctuations in $\rho(\mathbf{r})$ by some approximate procedure.[28,30]

There are several cases of practical interest where eq 1 reduces to a simplified form. First is the case where the structure consists of regions of electron density contrast arranged on a periodic lattice. Here, the scattering pattern will consist of a number of sharp peaks, and the application of Bragg's law will give the various lattice spacings. This type of analysis is entirely analogous to crystal structure determination by wide-angle X-ray diffraction. For structures without long-range periodicity, however, the calculation of a Bragg distance for a peak has little quantitative significance.[31]

The opposite extreme is a dilute system of particles dispersed in a matrix. In this case, correlations in phase between X-rays scattered by different particles are negligible and the observed scattered intensity is simply the sum of the scattered intensities from each of the particles. Thus, to calculate the scattering from a dilute system of identical particles, one must calculate the integral of eq 1 for a single particle and average over all particle orientations. For spherically symmetric particles, eq 1 reduces to[32]

$$I(q) = I_e(q) V \frac{1}{v_p} F^2(q) \quad (3)$$

where v_p is the average sample volume per particle and

$$F(q) = \int_0^\infty \rho(r) \frac{\sin(qr)}{qr} (4\pi r^2)\, dr \quad (4)$$

$F(q)$ is known as the structure factor of the particle. For a sphere of constant density

$$F(q) = v_0 \rho \Phi(qR) \quad (5)$$

where

$$\Phi(x) = 3\frac{\sin x - x\cos x}{x^3} \quad (6)$$

$$v_0 = \tfrac{4}{3}\pi R^3$$

and ρ is the electron density difference between the spheres and the matrix.

A third case, intermediate between these two, is characterized by a liquid-like degree of order in the relative positions of the particles. Zernike and Prins[33] have developed the scattering equations for such a system, and one form of their results[34] is

$$I(q) = I_e(q) V \frac{1}{v_p} F^2(q)\left\{1 - \frac{1}{v_p}\int_0^\infty [1 - P(r)]\frac{\sin(qr)}{qr}(4\pi r^2)\, dr\right\} \quad (7)$$

for spherically symmetric particles. $P(r)$ is related to the probability distribution function of interparticle separations and v_p is the average system volume per particle. Debye[35] assumed that for a system of hard spheres, $P(r) = 0$ for $r < 2R$ and $P(r) = 1$ for $r > 2R$ and showed that this leads to the result

$$I(q) = I_e(q) V \frac{1}{v_p} v_0^2 \rho^2 \Phi^2(qR)\left[1 - \frac{8v_0}{v_p}\Phi(2qR)\right] \quad (8)$$

Guinier argues[36] that Debye's approximation that $P(r)$ is independent of the particle concentration is inaccurate. This can clearly be seen in the fact that eq 8 predicts negative intensities for particle volume fractions (v_0/v_p) greater than about 0.125. Guinier suggested an equation derived by Fournet[37–39] based on the thermodynamic theory of Born and Green:[40]

$$I(q) = I_e(q) V \frac{1}{v_p} F^2(q) \frac{v_p}{v_p - (2\pi)^{3/2}\epsilon\beta(q)} \quad (9)$$

where ϵ is a constant very close to one and

$$\beta(q) = \frac{1}{q}\frac{2}{(2\pi)^{1/2}}\int_0^\infty r\alpha(r)\sin(qr)\, dr \quad (10)$$

where

$$\alpha(r) = e^{-\psi(r)/kT} - 1 \quad (11)$$

in which $\psi(r)$ is the interparticle potential function. For hard spheres, $\psi(r) = \infty$ for $r < 2R$ and $\psi(r) = 0$ for $r > 2R$. This approach then provides the following result for hard spheres:

$$I(q) = I_e(q) V \frac{1}{v_p} v_0^2 \rho^2 \Phi^2(qR) \frac{1}{1 + (8v_0/v_p)\epsilon\Phi(2qR)} \quad (12)$$

Another way to deal with systems with intermediate degrees of order is through a paracrystalline lattice model. In such a model, the scattering particles are arranged on a lattice that is disordered from perfect periodicity by allowing the lattice basis vectors to fluctuate in some way. This lattice disorder is referred to as disorder of the second kind. In addition, the particle positions and orientations in each lattice cell can fluctuate. This is referred to as disorder of the first kind. The mathematical analysis of these models is described in detail by Hosemann and Bagchi.[41] Unlike the Zernike–Prins-type model, the par-

acrystalline lattice approach can deal with particles and position distribution functions that are not spherically symmetric.

Here, we will consider a paracrystal having only disorder of the second kind. For this case, the scattered intensity is given by

$$I(\mathbf{q}) = I_e(\mathbf{q})V\frac{1}{v_c}F_c^2(\mathbf{q})Z(\mathbf{q}) \tag{13}$$

where v_c is the average volume per lattice cell, F_c is the structure factor of a lattice cell, and Z is the lattice statistics factor. If we wish to treat the sample as a collection of paracrystalline lattices that are randomly oriented, an average of eq 13 must be performed over all orientations of the vector $\mathbf{q}$. For simplicity, we will assume that the three average fundamental lattice vectors, $\langle\mathbf{a}_1\rangle$, $\langle\mathbf{a}_2\rangle$, and $\langle\mathbf{a}_3\rangle$, are orthogonal. We will further assume that the scattering particles are spheres of radius R and density ρ. For this case, the orientation averaging results in

$$I(q) = I_e(q)V\frac{2}{\pi v_c}\rho^2 v_0^2\Phi^2(qR)\int_0^{\pi/2}\int_0^{\pi/2}Z(q,\theta,\phi)\sin\theta\,d\theta\,d\phi \tag{14}$$

where θ and ϕ define the orientation of q with respect to the lattice coordinate system. In other words

$$\mathbf{q}\cdot\langle\mathbf{a}_1\rangle = q\langle a_1\rangle\sin\theta\cos\phi \tag{15}$$

$$\mathbf{q}\cdot\langle\mathbf{a}_2\rangle = q\langle a_2\rangle\sin\theta\cos\phi \tag{16}$$

$$\mathbf{q}\cdot\langle\mathbf{a}_3\rangle = q\langle a_3\rangle\cos\theta \tag{17}$$

For the case of an ideal paracrystal, in which all of the cells are parallelepipeds and the three lattice vectors fluctuate independently from cell to cell with a spherically symmetric Gaussian distribution about the mean, an analytical expression exists for $Z(\mathbf{q})$:

$$Z(\mathbf{q}) = \prod_{k=1}^{3}\mathrm{Re}\frac{1+F_k(\mathbf{q})}{1-F_k(\mathbf{q})} \tag{18}$$

where

$$F_k(\mathbf{q}) \cong |F_k(\mathbf{q})|\exp[-i(\mathbf{q})\cdot\langle\mathbf{a}_k\rangle] \tag{19}$$

and

$$|F_k(\mathbf{q})| \cong \exp[-\tfrac{1}{2}q^2 s_k^2] \tag{20}$$

where s is a measure of the breadth of the distribution of lattice vectors.

IV. Evaluation of Existing Models

In this section, through comparison of model calculations with the experimental data obtained on the sulfonated polystyrene ionomers, the strengths and weaknesses of each of the ionomer X-ray models will be examined. One of the features that will become an issue in the comparison of various models is the upturn in intensity near zero angle. It is not clear whether this feature is truly indicative of the structure resulting from ion aggregation or is simply artifact. In our data, the upturn occurs in the same region where the background scattering from the camera is strong. Thus, uncertainty in the measurement of the sample transmittance can have a strong effect on the result of the background subtraction procedure in this region. Another possible source of scattering near zero angle is sample impurities or voids. It should be noted that this feature of the curve has been widely observed even in pure polystyrene and in carboxylate ionomers in the acid form, where there is no evidence of ion aggregation and no SAXS peak.[14,42,49]

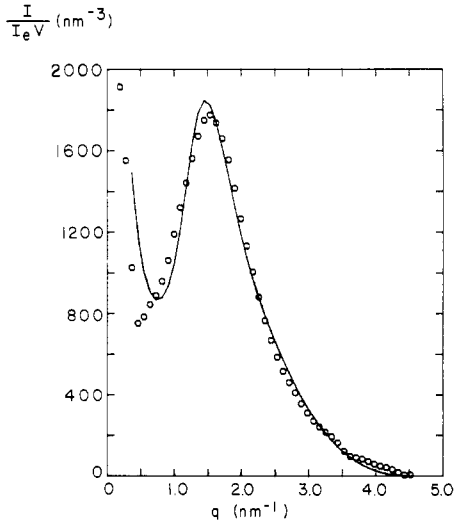

Figure 2. Fit of paracrystalline lattice model (solid line) to data for sample 4D (circles). The model parameters are a = 4.36 nm, s = 1.30 nm, R = 0.98 nm, and ρ = 133 nm^{-3}.

In our data, the characteristic ionomer SAXS peak was observed for all levels of neutralization, including the pure acid. This is contrary to the results of Peiffer et al.[49] on the same materials prepared by a slightly different procedure. For the evaluation of the various models, we will concentrate on the 85% neutralized salts.

There are two types of models that attribute the ionomer SAXS peak to an interparticle interference: the paracrystalline lattice models and the liquid-like interference models. The paracrystalline lattice is essentially the model used by Marx et al.[14] to analyze data obtained for a variety of ionomer systems. However, no attempt was made to calculate the scattering curve and compare it with the data. Using the apparent Bragg spacings and the known compositions of the samples, Marx et al. calculated that the number of ionic groups per aggregate ranges from 2 to 7 and increases as the overall ion content increases.

In considering the paracrystalline lattice approach, we chose to use a cubic lattice with equal disorder in all three basis vectors, i.e.

$$\langle a_1\rangle = \langle a_2\rangle = \langle a_3\rangle = a$$

and

$$s_1 = s_2 = s_3 = s$$

having identical spherical particles on each lattice point. Using eq 14–20, we attempted to fit the experimental SAXS curve for the zinc sulfonated polystyrene sample 4D. Considering the uncertainties in the region near zero angle, it was decided to fit only the data at q values greater than 0.5 nm^{-1}. Figure 2 shows the best fit as determined by nonlinear regression and the resulting model parameters. The model fits the data reasonably well but the calculated curve has a peak that is slightly sharper than that in the data. It is also important to check that the model parameters are reasonable, considering what is known about the sample composition. For this calculation, it is assumed that the number of sulfonate groups per unit volume of aggregate is given by the corresponding number for the zinc benzenesulfonate hexahydrate crystal structure[43] multiplied by the ratio of the apparent ionic phase electron density as determined by the model fit to that of the crystalline analogue. The electron density of the polystyrene matrix is 340 e$^-$/nm^3 and the electron density of zinc benzenesulfonate hexahydrate is 510 e$^-$/nm^3. The apparent ionic phase density is 340 + 133 = 473 e$^-$/nm^3.

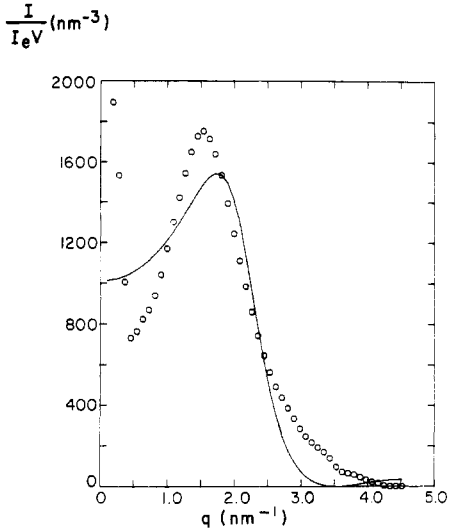

Figure 3. Fit of simple hard-sphere model (solid line) to data for sample 4D (circles). The model parameters are ρ = 34 nm^{-3}, R = 1.28 nm, and v_p = 20 nm^3.

In the crystal there are four sulfonate groups in each unit cell of 0.991 nm^3. Thus, from the model parameters, the apparent number of sulfonate groups in aggregates per unit volume of sample is

$$\frac{\frac{4SO_3}{0.991\ \text{nm}^3}\ \frac{473}{510}\ \frac{4}{3}\pi(0.98\ \text{nm})^3}{(4.36\ \text{nm})^3} = 0.18\ SO_3/\text{nm}^3$$

The actual concentration of sulfonate groups as determined by the density and mass function of sulfur for this sample is 0.42 SO_3/nm^3. Since the apparent number of ions in aggregates is less than the total available, there is no inconsistency with the known composition. The apparent fraction of ions in aggregates, β, for this model is 0.43.

One of the objections that is commonly raised against a paracrystalline lattice approach is that one has no rationalization based on physical arguments for the degree of correlation between ionic aggregate positions which the model implies. It would be more satisfying if one could derive the observed scattering from the Zernike–Prins liquid-like model with a physically reasonable postulate for the form of the interparticle potential function. The simplest such model involves the assumption of spherical particles that have no interaction other than impenetrability, i.e., a system of hard spheres. In evaluating this model, we will use eq 12. Some authors have used Debye's result (eq 8) but as was pointed out earlier, that approach is not accurate. As it turns out, the two equations can give curves of similar shape but the volume fraction of particles required is higher for the Fournet equation than for Deybe's equation for a given shape. This type of model is incapable of predicting the observed intensity upturn near zero angle but if an interparticle potential function with an attractive component is used, such a feature could be modeled.[44] Again, because of the uncertainties in that region, we have decided to use the simpler model and to fit only the data for q greater than 0.5 nm^{-1}. Figure 3 illustrates that this model could not provide a good fit. Futhermore, using the same type of calculation as for the paracrystalline lattice model, one finds that in this case there is an inconsistency with the known composition since the apparent concentration of sulfonate groups in aggregates is larger than the known total concentration by a factor of 3.

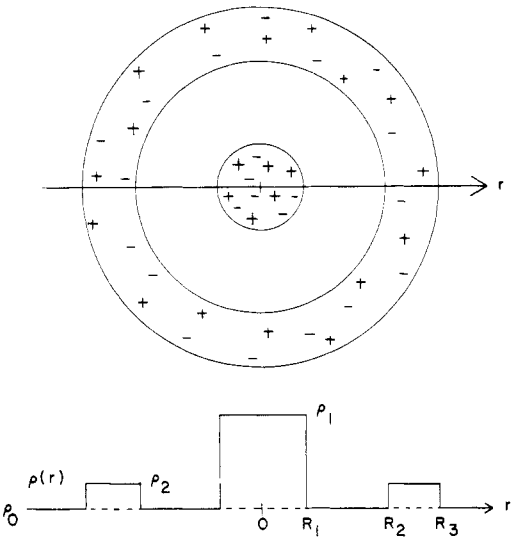

Figure 4. Original core–shell model and corresponding electron density profile.

Because of the deficiencies of the existing interparticle scattering models, other models have been proposed that attribute the ionomer SAXS peak to the internal structure of each ionic aggregate. Thus, they use the theory for dilute systems of particles. It is the particle structure factor that dictates the shape of the SAXS peak. The first model of this kind was proposed by MacKnight et al.[45] The ionic aggregate structure for this model is shown in Figure 4. The core is a dense aggregate of ionic groups surrounded by attached hydrocarbon chains. At some distance from the core is located a shell of ionic material at a significantly lower electron density than the core. The electron density distribution across the particle of this model is also shown in Figure 4. Using eq 3 and 4, one calculates for this model

$$I(q) = I_e(q)V\frac{1}{v_p}\left\{\frac{4\pi}{3}[\rho_1 R_1^3\Phi(qR_1) + \rho_2(R_3^3\Phi(qR_3) - R_2^3\Phi(qR_2))]\right\}^2 \quad (21)$$

Another model suggested by Roche et al.[22] involves a lamellar arrangement of three ionic regions with an electron density profile very similar to that in Figure 4. This model has very similar characteristics to the core–shell model when the averaging over all particle orientations is performed so it is not discussed in detail here. Fujimura et al.,[23] in referring to the core–shell model, use a different type of electron density profile. In this case, a central core of ionic material is surrounded by a shell that has been depleted of ions while the matrix has a finite ion concentration. This results in the profile shown in Figure 5. This model is much more intuitively appealing than the original core–shell model since it is difficult to imagine what forces could exist to maintain the shell of ions associated with the core over such distances. This is especially true when one considers the fact that the ionomer SAXS peak has been observed to persist in some cases to temperatures above 200 °C. The depleted-zone core–shell model is analogous to the structure that was originally thought to cause a similar SAXS peak in certain phase-separated metal alloys.[46] The resulting equation for this model is

$$I(q) = I_e(q)V\frac{1}{v_p}\left\{\frac{4\pi}{3}[(\rho_1 - \rho_2)R_1^3\Phi(qR_1) + \rho_2 R_2^3\Phi(qR_2)]\right\}^2 \quad (22)$$

Table II

sample	ρ_1, nm^{-3}	ρ_2, nm^{-3}	R_1, nm	R_2, nm	v_p, nm^3	β	γ	N
4A	170[a]	−0.7	1.00	3.4	1.0×10^3	0.16	0.15	17
4B	170[a]	−2.1	0.99	3.4	4.3×10^2	0.19	0.39	16
4C	170[a]	−3.5	1.03	3.3	2.8×10^2	0.20	0.52	18
4D	170[a]	−3.4	0.99	3.1	1.9×10^2	0.20	0.68	16

[a] Fixed during regression.

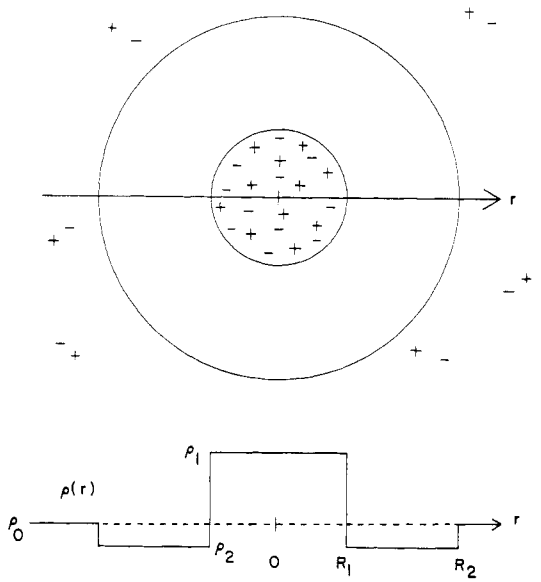

Figure 5. Depleted-zone core–shell model and corresponding electron density profile.

Both of these equations are capable of predicting an intensity upturn at very low angles but they do not fit the data very well as can be seen in Figure 6, where the results of nonlinear regression are shown along with the best-fit parameters. An improvement can be obtained by allowing for a distribution of dimensions. Using the depleted-zone version of the core–shell model and following the procedure of Fujimura et al.,[23] we allow for a normal distribution of core radii with a constant ratio of shell volume to core volume. If $P_r(R_1)$ is the probability of having an aggregate with radius R_1, we calculate the intensity as

$$I(q) = \int_0^\infty I(q,R_1)P_r(R_1)\,dR_1 \qquad (23)$$

$$P_r(R_1) = \frac{1}{\sigma\pi^{1/2}} \exp[(R_1 - \bar{R}_1)^2/\sigma^2] \qquad (24)$$

Figure 7 shows the results for this extension of the model. The fit is still not very good. If we ignore the very low angle data and fit only the region for which q is greater than 0.5 nm^{-1}, a reasonably good fit is obtained with the depleted-zone core–shell model even without a distribution of radii. In fact, allowing for a distribution does not improve the fit. Figure 8 shows the fits of this model to the entire series of data on the 85% neutralized salt of samples A, B, C, and D. Table II summarizes the best-fit parameters. For this type of model, v_p and the core electron density are not independent parameters so we have fixed ρ_1 at the electron density of zinc benzenesulfonate hexahydrate. The apparent fraction of sulfonate groups in aggregates, β, and the corresponding number of sulfonate groups per particle, N, are also listed in Table II. These values were determined by assuming that the number of sulfonates per unit volume of core is the same as in the crystalline analogue. Since these values are all less than one, the model is consistent with the sample composition. Also, since all the values of v_p are greater than $^4/_3\pi R_2^3$, there is no inconsistency with the assumption of a dilute system of particles.

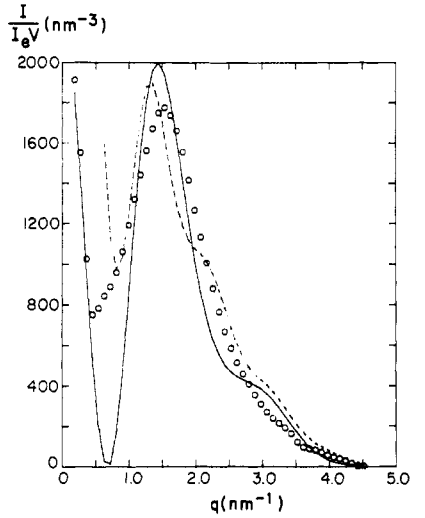

Figure 6. Attempted fits of original core–shell model (dotted line) and depleted-zone model (solid line) to entire range of data for sample 4D (circles). The model parameters are as follows. Original core–shell model: R_1 = 0.89 nm, R_2 = 3.6 nm, R_3 = 6.8 nm, ρ_1 = 170 nm^{-3}, ρ_2 = 3.8 nm^{-3}, v_p = 1.17 nm^3. Depleted-zone core–shell model: R_1 = 0.92 nm, R_2 = 3.81 nm, ρ_1 = 170 nm^{-3}, ρ_2 = −5.1 nm^{-3}, v_p = 169 nm^3.

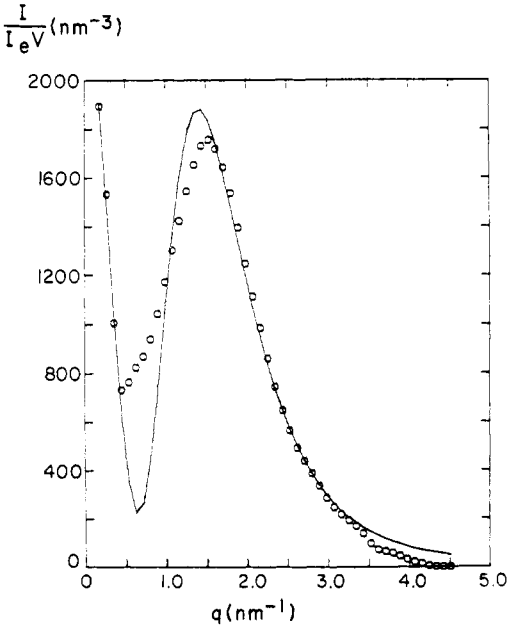

Figure 7. Fit of depleted-zone core–shell model with distribution of radii (solid line) to data for sample 4D (circles). The model parameters are R_1 = 0.51 nm, R_2 = 1.29 nm, σ = 0.66 nm, ρ_1 = 170 nm^{-3}, ρ_2 = −20 nm^{-3}, and v_p = 110 nm^3.

If the shell–core structure is formed by precipitation of ionic groups from the region enclosed by R_2, the number of ions in the aggregate should equal the original number in the region enclosed by R_2. Thus, the value of β as calculated should be equal to the ratio $(^4/_3\pi R_2^3)/v_p$, des-

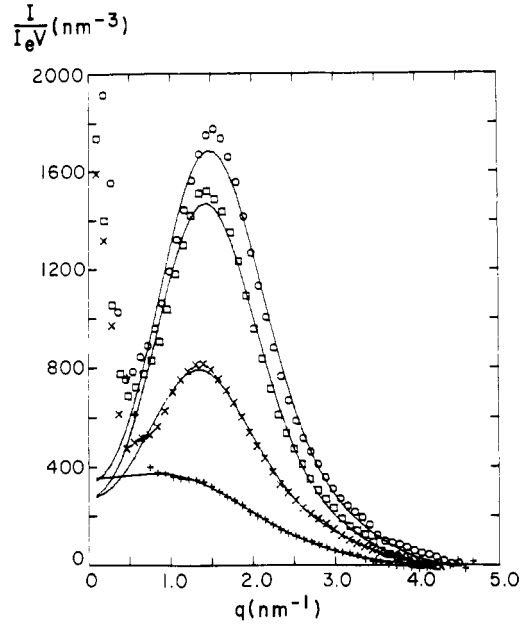

Figure 8. Fits of depleted-zone core–shell model (lines) to data for series 4 samples (symbols) ignoring data near zero angle.

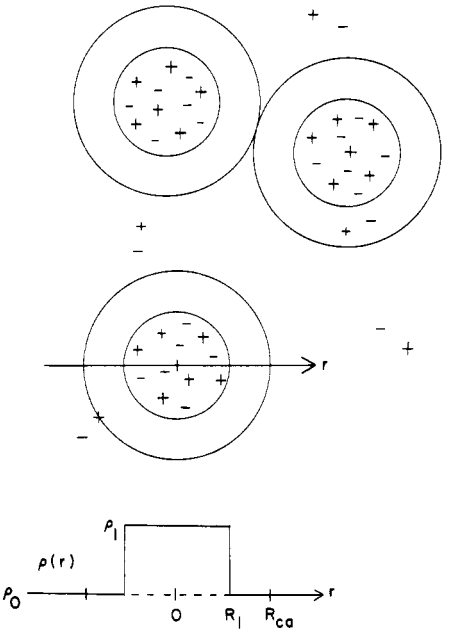

Figure 9. Schematic of modified hard-sphere model and corresponding electron density profile for one of the particles.

ignated γ. Those values are also listed in Table II. It is clear that the agreement here is not very good. Another discrepancy is that the values of ρ_2 are all about a factor of 5 smaller than one would expect assuming that the zone is completely depleted of ions and the matrix ion concentration is the same as the overall concentration. Finally, although the model curve has the right qualitative shape, the quantitative agreement near the peak is not very good.

V. Proposed Model

Of the existing models, the depleted-zone version of the core–shell model and the paracrystalline lattice model seem to be the most reasonable and agree best with available data. However, since even they are not entirely satisfactory, we decided to explore other possibilities. It was found that a slight variation on the hard-sphere liquid-like interference model has some very attractive characteristics. If it is postulated that the closest approach distance between two aggregates is $2R_{CA}$, where R_{CA} is greater than R_1, using eq 9–11 one can derive the relation

$$I(q) = I_e(q)V\frac{1}{v_p}v_1^2\rho_1^2\Phi^2(qR_1)\frac{1}{1 + (8v_{CA}/v_p)\epsilon\Phi(2qR_{CA})} \quad (25)$$

where $v_{CA} = {}^4/_3\pi R_{CA}^3$ and $v_1 = {}^4/_3\pi R_1^3$. This reduces to eq 12 if $R_{CA} = R_1$. Physically, it is expected that each ionic aggregate must necessarily be coated with an attached layer of hydrocarbon material whose electron density is the same as the matrix but which would provide a steric limitation on the relative positions of two ionic aggregates. This model is shown schematically in Figure 9. Using eq 25 and again ignoring the very low angle data, we find that all the data for the zinc sulfonated polystyrene system can be fit extremely well. In initial trials with all of the parameters free to vary, the resulting value of ρ_1 did not change significantly through the series of sulfonation levels with a constant degree of neutralization. Since the aggregate composition was expected to depend only on the chemical nature of the cation–anion pair and not on the overall ion concentration, it was decided to fix the value of ρ_1 for samples A, B, and C at the value determined by the fit for sample D in each series. The matrix electron density, in principle, depends on the amount of ionic

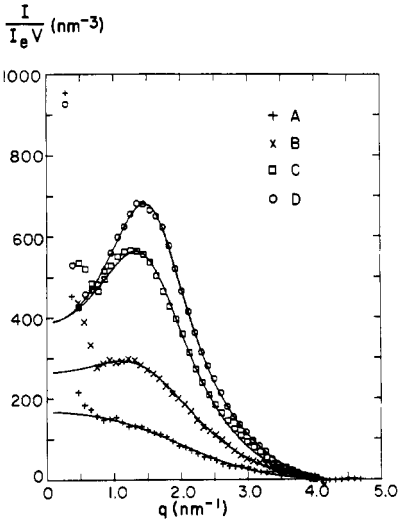

Figure 10. Fits of modified hard-sphere model (lines) to data for SPS acid (series 1) samples (symbols).

material that is not contained in aggregates. However, calculations indicate that at the sulfonation levels used, the highest matrix electron density possible even with all of the ionic units dissolved in the matrix in the most concentrated sample is 360 e^-/nm^3. Since the density for pure polystyrene is 340 e^-/nm^3, this effect was ignored. Figure 10–13 show the fits for all of the samples. Table III lists the best-fit parameters. Using the same approach employed in the analysis of the simple hard-sphere model, we calculated the fraction of ionic groups that are in aggregates, β, as well as the number of sulfonate groups per aggregate, N. For the acid samples, the crystal structure of *p*-toluenesulfonic acid monohydrate[47] was used to determine the appropriate density of sulfonate groups in the aggregates. The electron density of this crystal analogue is 460 e^-/nm^3. For the partially neutralized materials, a weighted average of the density in the two crystal analogues was used. Since none of the values of β are greater than one, it is apparent that this model is consistent with the sample compositions. From examination of Table III, it is clear that these data imply that there is no significant change in the aggregate structure or characteristic di-

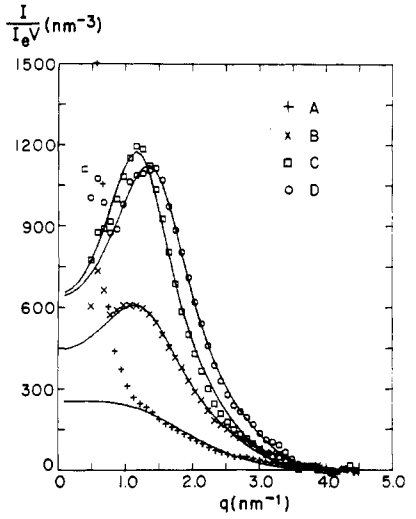

Figure 11. Fits of modified hard-sphere model (lines) to data for 25% neutralized ZnSPS (series 2) samples (symbols).

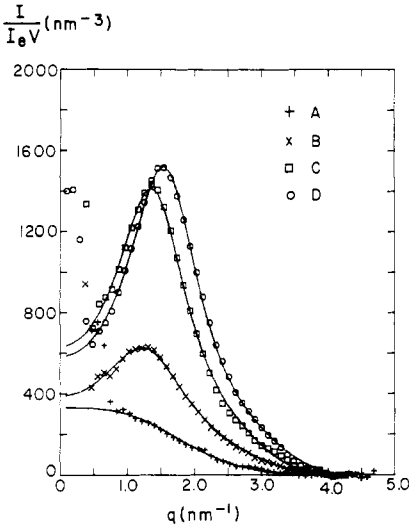

Figure 12. Fits of modified hard-sphere model (lines) to data for 50% neutralized ZnSPS (series 3) samples (symbols).

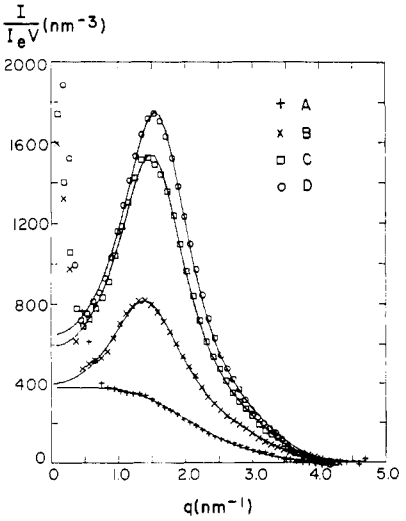

Figure 13. Fits of modified hard-sphere model (lines) to data for 85% neutralized ZnSPS (series 4) samples (symbols).

mensions with ion content but only a change in the concentration of aggregate particles. Interestingly, the values for the number of ionic groups per aggregate and the insensitivity of that parameter to the overall ion content are

Table III

sample	ρ_1, nm^{-3}	R_1, nm	R_{CA}, nm	v_p, nm^3	β	N
1A	70[a]	0.98	1.2	3.9×10^2	0.41	16
1B	70[a]	0.99	1.53	1.9×10^2	0.43	17
1C	70[a]	1.04	1.65	1.3×10^2	0.45	19
1D	70	1.01	1.62	8.9×10^1	0.47	18
2A	87[a]	1.07	1.7[a]	6.0×10^2	0.32	19
2B	87[a]	1.09	1.91	2.6×10^2	0.39	20
2C	87[a]	1.16	2.08	2.1×10^2	0.35	25
2D	87	1.07	1.77	1.2×10^2	0.39	19
3A	85[a]	1.11	1.7[a]	6.7×10^2	0.30	21
3B	85[a]	1.05	1.91	2.0×10^2	0.43	17
3C	85[a]	1.08	1.85	1.0×10^2	0.57	19
3D	85	1.00	1.67	6.2×10^1	0.59	15
4A	89[a]	1.02	1.5	3.0×10^2	0.49	15
4B	89[a]	0.98	1.78	1.1×10^2	0.59	13
4C	89[a]	1.00	1.73	7.0×10^1	0.62	14
4D	89	1.00	1.66	5.8×10^1	0.59	14

[a] Fixed during regression. Note: The value of R_{CA} primarily affects the peak position. Since, in the low ion content materials, the peak is weak or nonexistent, the value of R_{CA} contains considerable uncertainty for these materials. In two cases, the value had to be fixed arbitrarily in order for the regression procedure to converge.

quite consistent with the predictions of Forsman from statistical mechanical calculations.[48]

From the apparent electron density difference between the aggregates and the matrix and the known density of the matrix, it appears that the ionic domains in the acid samples are 9% less dense than crystals of toluenesulfonic acid monohydrate. In the 85% neutralized salt, the domains are about 10% less dense than zinc benzenesulfonate hexahydrate crystals. These numbers seem reasonable and imply a fairly well-ordered structure within the aggregates, in agreement with extended X-ray absorption fine structure data obtained by us on these materials.[26] This model can also explain the persistence of the SAXS peak to high temperatures because these crystal-like aggregates would be expected to be quite stable.

It should be pointed out that the values for the aggregate size and concentration as determined from this model are in excellent agreement with those resulting from the paracrystalline lattice model. It is apparent that the actual physical situations represented by the two models with the values of the parameters that were determined are nearly identical. The advantages of the liquid-like model are that there is a physical rationalization for the correlation in particle positions and that the acutal degree of order that exists can be modeled more accurately with the liquid-like approach than with the ideal paracrystal.

The only deficiency of this model is its inability to predict the intensity scattered at very low q. However, as discussed previously, none of the existing models can adequately fit that region either. The uncertainties in the data in that region have also been described.

It has been argued[22,23] that any model that attributes the scattering peak to an interparticle interference is necessarily inconsistent with the observed shifts in peak position as a function of swelling or elongation which were discussed in the Introduction. It has been said that if the peak is due to interparticle interference, the apparent Bragg spacing should change in proportion to the macroscopic dimension changes, contrary to what has been observed. However, these arguments are based on the assumption that the total number of aggregates and the number of ionic groups per aggregate remain the same during the deformation or swelling process. We believe

it is very unlikely that this is the case. Let us consider deformation first. Using the 6.9% sulfonated material as an example, one finds that the average contour length between ions participating in aggregates along a chain is 6.2 nm. The average distance between domains in the undeformed sample, taken as $v_p^{1/3}$, is 3.9 nm. Thus at a 60% strain level, the average chain will be stretched to its contour length, and further deformation must result in either chain rupture or aggregate rupture. Because of the distribution of subchain lengths, one might expect significant reorganization of the domains even at very low strains. This could be tested by measuring the elastic recovery of an ionomer when strained above the backbone glass transition temperature. In an experiment where the ionic domains are swelled by water, one might expect that the number of ionic groups per unit area of the water micelle would remain roughly constant. This would require coalescence of different domains during swelling and would be consistent with the data. We intend to test these postulates in future experiments.

Several spectroscopic studies[8-11] have indicated the existence of more than one kind of environment for the ionic groups in ionomers. These have usually been interpreted in terms of the "multiplets" and "clusters" proposed by Eisenberg. Examining these data in terms of the proposed model suggests that the two environments may correspond to ions dispersed in the matrix and ions in the aggregates. The dispersed ionic groups probably exist as a zinc atom coordinated by two sulfonate groups. In fact, it seems more reasonable that these two situations should manifest themselves in different infrared and Raman vibration frequencies than the multiplet and cluster environments. There is actually little difference in the local ionic environment between the multiplet and cluster states, and it is the local environment that primarily affects the bond vibration frequencies. Since the aggregate environment of the proposed model is close to that in an ionic crystal, it is reasonable to expect different vibration energies for these ions compared to ionic groups isolated in the matrix.

The results of the present analysis also indicate no transition in structure as a function of ion content. This is in contrast to some of the work of Eisenberg,[4,15] which shows the breakdown of time–temperature superposition and a sudden shift in the apparent Bragg spacing at a composition of about 6% methacrylic acid in styrene/methacrylic acid copolymers. However, Raman spectroscopy studies of Eisenberg et al.[9] and other spectroscopic studies[10,11] also indicate no transition in the structure but simply a change in the relative populations of the two ion environments.

The apparent Bragg spacing shift is reported by Eisenberg only for the Cs^+-neutralized materials, where d_B changes from about 2.0 nm to about 6.0 nm at a methacrylic acid content of about 6%. No such change is observed in Li^+- or Na^+-neutralized samples. The Cs^+ data conflict with data obtained by Roche[42] on the same materials. He observes no SAXS peak in the low ion content materials, and in the 7.7 and 9.7% materials, d_B is about 3.0 nm. Thus, it appears that the structure of Cs^+ salts of styrene/methacrylic acid ionomers may be very sensitive to the sample preparation method.

The applicability of the time–temperature superposition principle requires that all of the relaxation processes have the same temperature dependence. In ionomers, an important relaxation mode must involve the pulling of ionic groups from an aggregate. There is no reason to expect this mode to behave in the same way as the polystyrene backbone relaxations. Thus, it is not surprising that superposition does not work for high ion content ionomers. The fact that it does seem to work for low ion content materials may be due to the fact that there is simply not enough ionic material for the effects of that relaxation mode to be observable.

VI. Conclusions

A modified hard-sphere scattering model is proposed that is consistent with much of the existing SAXS data on ionomers and is capable of quantitatively modeling the characteristic SAXS peak in sulfonated polystyrene ionomers. The model provides a better fit than any existing model and its physical interpretation is straightforward. If the model is valid, it implies that in the Zn^{2+}-neutralized sulfonated polystyrene system, about half of the ionic groups are aggregated in well-ordered domains with the remainder dispersed in the matrix. The ionic domains are about 2.0 nm in diameter and contain about 20 sulfonate units. The layer of attached polystyrene chains on the surface of each aggregate prevents any two aggregates from being closer than about 3.4 nm center to center. There is no change in the aggregate structure or size as a function of ion content; the change in the SAXS pattern is due to a change in the concentration of aggregate particles.

Acknowledgment. This research was performed in part at the National Center for Small-Angle Scattering Research at Oak Ridge National Laboratory. We appreciate very much the help of Dr. J. S. Lin and Dr. R. W. Hendricks in using the NCSASR facility. Partial support of this research by the polymers section of the NSF Division of Materials Research through Grant DMR 81-06888 and the Department of Energy through Contract DE-AC02-81ER 10922 is gratefully acknowledged.

References and Notes

(1) R. Longworth, in "Ionic Polymers", L. Holliday, Ed., Applied Science Publishers, London, 1975, Chapter 2.
(2) "Perfluorocarbon Ion Exchange Membranes", Papers presented at the 152nd Meeting of the Electrochemical Society, Atlanta, 1977.
(3) W. J. MacKnight and T. Rr. Earnest, Jr., *J. Polym. Sci., Macromol. Rev.*, **16**, 41 (1981).
(4) A. Eisenberg and M. King, "Ion Containing Polymers: Physical Properties and Structure", Academic Press, New York, 1977.
(5) L. Holliday, Ed., "Ionic Polymers", Applied Science Publishers, London, 1975.
(6) A. Eisenberg, in "Contemporary Topics in Polymer Science", M. Shen, Ed., Plenum Press, New York, 1979, Vol. 3, p 231.
(7) A. Eisenberg, *Macromolecules*, **3**, 147 (1970).
(8) I. M. Hodge and A. Eisenberg, *Macromolecules*, **11**, 289 (1978).
(9) A. Neppel, I. S. Butler, and A. Eisenberg, *J. Polym. Sci., Polym. Phys. Ed.*, **17**, 2145 (1979).
(10) E. D. Andreeva, V. N. Nikitin, and Yu. M. Boyartchuk, *Macromolecules*, **9**, 238 (1976).
(11) G. B. Rouse, W. M. Risen, A. T. Tsatsas, and A. Eisenberg, *J. Polym. Sci., Polym. Phys. Ed.*, **17**, 81 (1979).
(12) R. Longworth and D. J. Vaughn, *Nature (London)*, **218**, 85 (1968).
(13) J. Kao, R. S. Stein, W. J. MacKnight, W. P. Taggart, and G. S. Cargill III, *Macromolecules*, **7**, 95 (1974).
(14) C. L. Marx, D. F. Caulfield, and S. L. Cooper, *Macromolecules*, **6**, 344 (1973).
(15) A. Eisenberg and M. Navratil, *Macromolecules*, **7**, 90 (1974).
(16) M. Pineri, C. Meyer, A. M. Levelut, and M. Lambert, *J. Polym. Sci., Polym. Phys. Ed.*, **12**, 115 (1974).
(17) E. J. Roche, R. S. Stein, and W. J. MacKnight, *J. Polym. Sci., Polym. Phys. Ed.*, **18**, 1035 (1980).
(18) T. R. Earnest, Jr., J. S. Higgins, D. L. Handlin, and W. J. MacKnight, *Macromolecules*, **14**, 192 (1981).
(19) T. D. Gierke, G. E. Munn, and F. C. Wilson, *J. Polym. Sci., Polym. Phys. Ed.*, **19**, 1687 (1981).
(20) M. Fujimura, T. Hashimoto, and H. Kawai, *Macromolecules*, **14**, 1309 (1981).
(21) E. Roche, M. Pineri, R. Duplessix, and A. Levelut, *J. Polym. Sci., Polym. Phys. Ed.*, **19**, 1 (1981).

(22) E. J. Roche, R. S. Stein, T. P. Russell, and W. J. MacKnight, *J. Polym. Sci., Polym. Phys. Ed.*, **18**, 1497 (1980).
(23) M. Fujimura, T. Hashimoto, and H. Kawai, *Macromolecules*, **15**, 136 (1982).
(24) R. D. Lundberg, H. S. Makowski, and L. Westerman, U.S. Patent 4 014 847 (Mar 29, 1977) to Exxon Research and Engineering Co.
(25) H. S. Makowski, R. D. Lundberg, and G. H. Singhal, U.S. Patent 3 870 841 (Mar 11, 1975) to Exxon Research and Engineering Co.
(26) D. J. Yarusso, H. K. Pan, and S. L. Cooper, to be published.
(27) I. Pilz, *J. Colloid Interface Sci.*, **30**, 140 (1969).
(28) J. Rathje and W. Ruland, *Colloid Polym. Sci.*, **254**, 358 (1976).
(29) A. Guinier and G. Fournet, "Small Angle Scattering of X-rays", Wiley, New York, 1955.
(30) G. Kortleve, C. A. F. Tuynman, and C. G. Vonk, *J. Polym. Sci., Part A-2*, 123 (1972)
(31) Reference 29, p 140.
(32) Reference 29, p 10.
(33) F. Zernike and J. A. Prins, *Z. Phys.*, **41**, 184 (1927).
(34) Reference 29, p 35.
(35) P. Debye, *Phys. Z.*, **28**, 135 (1927).
(36) Reference 29, pp 41, 44.
(37) G. Fournet, *C. R. Hebd. Seances Acad. Sci.*, **228**, 1421 (1949).
(38) G. Fournet, *C. R. Hebd. Seances Acad. Sci.*, **229**, 1071 (1949).
(39) G. Fournet, *Acta Crystallogr.*, **4**, 293 (1951).
(40) M. Born and H. S. Green, *Proc. R. Soc. London, Ser. A*, **188**, 10 (1946).
(41) R. Hosemann and S. N. Bagchi, "Direct Analysis of Diffraction by Matter," North-Holland, Publishing Co., Amsterdam, 1962.
(42) E. J. Roche, Ph.D. Thesis, Polymer Science and Engineering Department, University of Massachusetts, 1978.
(43) J. M. Broomhead and A. D. I. Nicol, *Nature (London)*, **160**, 795 (1947).
(44) Reference 29, p 49.
(45) W. J. Macknight, W. P. Taggart, and R. S. Stein, *J. Polym. Sci., Polym. Symp.* **No. 45**, 113 (1974).
(46) C. B. Walker and A. Guinier, *C. R. Hebd. Seances Acad. Sci.*, **234**, 2379 (1952).
(47) S. K. Arora and M. Sundaralingam, *Acta Crystallogr. Sect. B*, **27**, 1293 (1971).
(48) W. C. Forsman, *Macromolecules*, **15**, 1032 (1982).
(49) D. G. Peiffer, R. A. Weiss, and R. D. Lundberg, *J. Polym. Sci., Polym. Phys. Ed.*, **20**, 1503 (1982).

Short-Range Order in Form II of Poly(vinylidene fluoride): Antiphase Domain Structures

Yasuhiro Takahashi* and Hiroyuki Tadokoro

Faculty of Science, Department of Macromolecular Science, Osaka University, Toyonaka, Osaka 560, Japan. *Received February 24, 1983*

ABSTRACT: The crystal structure of form II of poly(vinylidene fluoride) was reported to include the disorder that four molecules with different orientation occupy a crystal site with different existence probabilities. In the present study, it is established that there exists a short-range order, antiphase domain structures, in the crystallite of form II. The antiphase domain structures on the *c* projection and for the up and down molecules explain the half-widths of two series of the reflections: 120, 130, 140, and 011, 021, 031, respectively. In the antiphase domain structure on the *c* projection, the size of a domain is much longer in the *a* direction than in the *b* direction, while, in the antiphase domain structure for the up and down molecules, the size of a domain in the *a* direction is considered to be comparable to that in the *b* direction. From the antiphase domain structures, it is concluded that the locally stable structure of form II is the antipolar and antiparallel structure.

In previous papers,[1-4] it was established that a conformational disorder, a kink band, exists in form I and streak II of poly(vinylidene fluoride), and it was reported that the conformational disorder plays an important role in the crystal phase transformation. On the other hand, it is also very interesting to clarify what kind of disorder with respect to the molecular packing exists in the crystalline region. In the preceding paper,[5] the crystal structure of form II was analyzed in detail. The analysis showed that four molecules with different orientation statistically coexist at a crystal site with different existence probabilities (Figure 1). Among two series of reflections $1k0$: 120, 130, 140, and $0k1$: 011, 021, 031, the superlattice spots with $h + k = 2n + 1$ were much broader than the reflections with $h + k = 2n$. This suggests that there exists a short-range order in the crystalline region. The purpose of the present study is to clarify what kind of short-range order exists in the crystalline region and what structure is locally stable in form II.

Experimental Section

The poly(vinylidene fluoride) sample used for this study is KF-1100 (Kureha Chemical Industry Co., Ltd.). A uniaxially oriented sample was prepared by stretching at 150 °C, followed by annealing at 175 °C for 24 h. X-ray measurements were made with Cu Kα radiation monochromatized by a graphite monochromator. Fiber photographs were taken in a He gas atomosphere with a cylindrical camera with a 5-cm radius. Intensity was digitally measured by a drum scanner (Optronics) installed in the Crystallographic Research Center of this University. The digital data were summed along each reflection arc after the density was converted to the intensity. The profiles of the reflections 120, 130, 011, 021, and 031 are plotted along the layer lines in Figure 2, where the reflections 021 and 031 are separated from the reflections 111 and 121 by assuming a Gaussian distribution, respectively.

Antiphase Domain Structure on the *c* Projection

From the crystal structure (Figure 1), the reflections with $h + k$ = odd for hkl correspond to the so-called "superlattice spots".[6] On the equator, the half-widths of the reflections 120, 130, and 140 are found to be broad, very sharp, and broad, respectively (Figure 2).[5] This relation in half-width cannot be interpreted by the anisotropy in the crystallite size and disorder of the second kind.[7] It should be rather considered that there exists a short-range order in packing of the molecules with different orientation A and $\bar{A}$ (Figure 3) on the *c* projection. In comparison with reflections of other crystalline polymers, the reflections 120 and 140 are not so broad. This suggests that the short-range order on the *c* projection is very regular. Accordingly, a domain structure is reasonably considered for the short-range order. Furthermore, the intermolecular distance calculated for the crystal structure[5] requires that the molecules aligned along the *a* axis have the same orientation A or $\bar{A}$. Accordingly, the size of a domain is considered to be very long in the *a* direction and could be assumed to be infinite in the *a* direction, while the size in

0024-9297/83/2216-1880$01.50/0